Water Research 148 (2019) 41–50

Contents lists available at ScienceDirect

Water Research

journal homepage: www.elsevier.com/locate/watres

Comprehensive retention model for PFAS transport in subsurface systems

Mark L. Brusseau [a, b, *], Ni Yan [b], Sarah Van Glubt [a], Yake Wang [a], Wei Chen [a], Ying Lyu [a, c], Barry Dungan [d], Kenneth C. Carroll [d], F. Omar Holguin [d]

[a] Soil, Water, and Environmental Science Department, University of Arizona, Tucson, AZ, 85721, United States
[b] Hydrology and Atmospheric Sciences Department, University of Arizona, Tucson, AZ, 85721, United States
[c] Institute of Water Resources and Environment, Jilin University, Changchun, 130026, PR China
[d] Department of Plant & Environmental Sciences, New Mexico State University, Las Cruces, NM, United States

ARTICLE INFO

Article history:
Received 30 May 2018
Received in revised form
12 October 2018
Accepted 12 October 2018
Available online 15 October 2018

Keywords:
PFAS
PFOA
PFOS
Air-water interfacial adsorption
Retardation

ABSTRACT

A comprehensive compartment model is presented for PFAS retention that incorporates all potential processes relevant for transport in source zones. Miscible-displacement experiments were conducted to investigate separately the impact of adsorption at the air-water and decane-water interfaces on PFAS retention and transport. Two porous media were used, a quartz sand and a soil, and perfluorooctanesulfonic acid (PFOS) was used as the model PFAS. The breakthrough curves for transport under water-unsaturated conditions were shifted noticeably rightward (delayed arrival) compared to the breakthrough curves for saturated conditions, indicating greater retardation due to adsorption at the air-water or decane-water interface. The retardation factor was 7 for PFOS transport in the sand for the air-water system, compared to 1.8 for saturated conditions. PFOS retardation factors for transport in the soil were 7.3 and 3.6 for unsaturated (air-water) vs saturated conditions. Air-water interfacial adsorption is a significant source of retention for PFOS in these two systems, contributing more than 80% of total retention for the sand and 32% for the soil. For the experiments conducted with decane residual emplaced within the sand, adsorption at the decane-water interface contributed more than 70% to total retention for PFOS transport. Methods to determine or estimate key distribution variables are presented for parameterization of the model. Predicted retardation factors were similar to the measured values, indicating that the conceptual model provided adequate representation of the relevant retention processes and that the parameter estimation methods produced reasonable values. The results of this work indicate that adsorption by fluid-fluid interfaces in variably saturated porous media can be a significant retention process for PFAS that should be considered when characterizing their transport and fate behavior in source zones.

1. Introduction

Per- and poly-fluoroalkyl substances (PFAS) have become critical emerging contaminants of concern. Recent research has shown that they are widespread in the environment (Rayne and Forest, 2009; Ahrens, 2011; Krafft and Riess, 2015; Cousins et al., 2016). A lifetime health advisory of 0.07 μg/L was issued by the US EPA in 2016 for the combined total of perfluorooctanesulfonic acid (PFOS) and perfluorooctanoic acid (PFOA), two primary PFAS of concern, for long-term exposure through drinking water (EPA, 2016). The observed concentrations of PFOS and PFOA in groundwater are often orders of magnitude greater than the health advisory value (Moody and Field, 1999, Moody et al., 2003; Rayne and Forest, 2009; Ahrens, 2011; Anderson et al., 2016; Cousins et al., 2016). Thus, the occurrence of PFAS in soil and groundwater and the resultant potential implications for human exposure are of significant interest and concern.

Robust determination of the risks posed by PFAS contamination of soil and groundwater, as well as the development and implementation of effective remediation strategies, requires an accurate understanding of PFAS transport and fate behavior in the

* Corresponding author. Soil, Water, and Environmental Science Department, University of Arizona, Tucson, AZ, 85721, United States.
E-mail address: brusseau@email.arizona.edu (M.L. Brusseau).

https://doi.org/10.1016/j.watres.2018.10.035
0043-1354/

subsurface. Many of the critical PFAS of concern, such as PFOS and PFOA, are highly recalcitrant. Hence, retention (phase distribution) will typically be the primary process influencing transport and fate of these PFAS. Sorption by the solid phase of porous media is a primary retention process, and has been a focus of research over the past decade for PFAS. Solid-phase sorption of PFAS is generally anticipated to be the sole source of retardation for transport within groundwater contaminant plumes. However, additional retention processes are likely to influence PFAS transport in source zones (Brusseau, 2018; Lyu et al., 2018).

Given that many PFAS of concern are surfactants, adsorption at the air-water interface is one retention process that may be relevant for PFAS transport in vadose-zone systems. Recent in-depth characterizations of the occurrence and fate of PFAS at field sites have demonstrated that vadose-zone sources are a primary subsurface reservoir of PFAS, serving as long-term sources to groundwater (Shin et al., 2011; Xiao et al., 2015; Weber et al., 2017). This indicates that understanding PFAS transport and fate behavior in vadose-zone systems is critical. The potential significance of air-water interfacial adsorption for PFOS and PFOA transport and retardation was illustrated in recent theoretical and experimental analyses (Brusseau, 2018; Lyu et al., 2018).

Another set of retention processes that may be relevant for PFAS transport in source zones is partitioning to bulk phases of immiscible organic liquids (NAPL) and to interfaces between NAPL and aqueous solution. It has been demonstrated that PFAS can co-occur with NAPL at certain types of sites, such as fire training areas (e.g., Moody et al., 2003; McGuire et al., 2014). Thus, it is anticipated that NAPL-water partitioning and NAPL-water interfacial adsorption may influence PFAS transport and retardation in such settings. The results of a few prior studies indicate an impact of these processes on PFAS retention (Chen et al., 2009; Guelfo and Higgins, 2013; McKenzie et al., 2016). However, the specific, discrete impacts of partitioning versus interfacial adsorption were not differentiated. The discrete impacts of both processes, in addition to air-water interfacial adsorption, was examined in the recent theoretical analysis by Brusseau (2018).

Current conceptual and mathematical models of PFAS transport and fate in the subsurface focus on solid-phase sorption as the sole source of retention. For example, all three of the detailed characterizations of field-scale PFAS transport and fate discussed above employed this assumption. In addition, this assumption is present in recent comprehensive reports on PFAS management (CONCAWE, 2017; CRCCARE, 2017; NGWA, 2017). While this approach is sufficient for characterizing transport within groundwater contaminant plumes, it is likely to be inadequate for representing transport in source zones.

We present a comprehensive compartment model for PFAS retention that incorporates all potentially relevant processes. Methods to determine or estimate key distribution variables are presented to parameterize the model. The effectiveness of the model is tested for two specific cases, one with solid-phase sorption and air-water interfacial adsorption and another with solid-phase sorption and adsorption at the NAPL-water interface.

2. Conceptual model and parameter determination

2.1. Conceptual model

Compartment models have long been employed for characterizing the distribution of contaminants in environmental media. A modified 14-compartment model was recently developed for PFAS (NGWA , 2017). It is focused on differentiating the behavior of anionic, cationic, and zwitterionic species. The model includes aqueous, sorbed (solid phase), and vapor phases, but does not include partitioning to NAPL or adsorption at fluid-fluid interfaces. Brusseau (2018) presented a multi-process conceptual model for PFAS retention that included adsorption at the air-water interface, partitioning to the soil atmosphere, adsorption at the NAPL-water interface, and partitioning to NAPL in addition to solid-phase adsorption. This model is extended herein in terms of a multi-compartment model as shown in Fig. 1. The compartments are divided between source zones and plumes in recognition of differential retention behavior between the two regions. Note that the source zone includes the vadose zone as well as saturated-zone regions. Similarly, the plume compartments represent the groundwater contaminant plume and the vadose-zone region above the plume. Furthermore, it is noted that the aqueous phase for both regions includes dissolved PFAS as well as PFAS that may be associated with suspended or dissolved colloidal matter. The phases are color-coded based on posited likelihood of general relevance.

The retardation factor (R) for aqueous-phase transport of solute undergoing retention by all of the processes depicted in Fig. 1 is given as:

$$R = 1 + K_d\rho_b/\theta_w + K_a\theta_a/\theta_w + K_{aw}A_{aw}/\theta_w + K_n\,\theta_n/\theta_w + K_{nw}A_{nw}/\theta_w + K_{an}A_{an}/\theta_w \quad (1)$$

where K_d is the solid-phase adsorption coefficient (cm^3/g), K_n is the NAPL-water partition coefficient (−), K_a is the air-water partition coefficient (Henry's coefficient, -), K_{aw} is the air-water interfacial adsorption coefficient (cm^3/cm^2), K_{nw} is the NAPL-water interfacial adsorption coefficient (cm^3/cm^2), K_{an} is the air-NAPL interfacial adsorption coefficient (cm^3/cm^2), A_{aw} is the specific air-water interfacial area (cm^2/cm^3), A_{nw} is the specific NAPL-water interfacial area (cm^2/cm^3), A_{an} is the specific air-NAPL interfacial area (cm^2/cm^3), ρ_b is porous-medium bulk density (g/cm^3), θ_a is volumetric air content (−), θ_n is volumetric NAPL content (−), and θ_w is volumetric water content (−). By phase balance, $\theta_w + \theta_a + \theta_n = n$, where n is porosity.

2.2. Parameter determination

The model requires input values for all of the terms in equation (1) to produce a predicted R. The parameter determination approach developed herein is designed to provide telescoping predictions that increase in accuracy based on the level of input information available to the user. To accomplish this, each input parameter has multiple source modes, based on estimation refinement. The highest accuracy mode is the availability of a measured value. Absent a measured value, relevant methods for estimation of that specific parameter are used. This approach is delineated in Table 1.

Multiple methods are available for estimating distribution/partition coefficients. For example, empirical approaches based on linear free energy relationships (LFER) and quantitative-structure/property relationships (QSPR) can be employed to estimate partition coefficients. In addition, semi-empirical methods such as UNIFAC and SPARC models are available. These approaches have been widely used to determine phase-distribution coefficients for many different compounds, including PFAS (e.g., Arp et al., 2006; Goss et al., 2006; Bhhatarai and Gramatica, 2011). For example, Bhhatarai and Gramatica conducted an extensive QSPR analysis for PFAS, and showed that aqueous solubility, vapor pressure, and CMC (critical micelle concentration) were all well described by simple QSPR models. Lyu et al. (2018) presented a QSPR model to predict air-water interfacial adsorption coefficients for PFAS.

Standard methods widely used to measure or estimate values for ρ_b, n, θ_w, θ_a, and θ_n can be employed. The estimation methods for the other parameters are discussed briefly below.

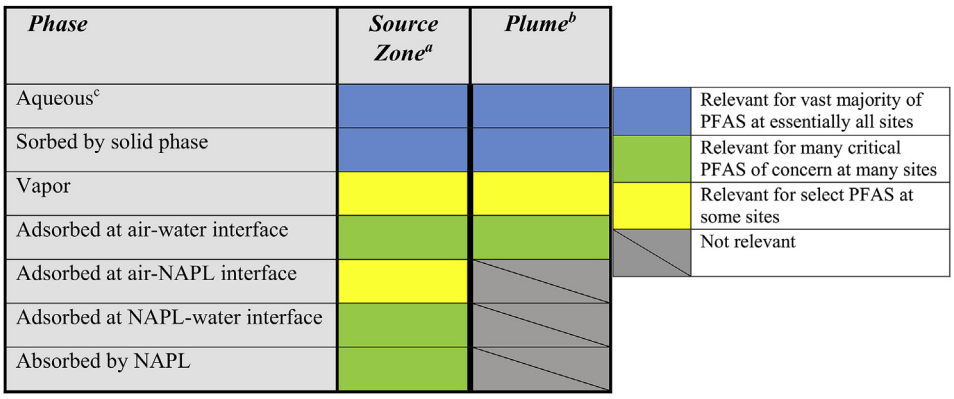

Fig. 1. Comprehensive compartment model for PFAS retention.

Table 1
Tiered methods for measuring and estimating model input parameters.

Parameter	Method 1	Method 2	Method 3
K_d	Measured for specific PFAS and soil	Estimated using advanced solid-phase adsorption model, with measured soil components	Estimated using K_{oc}-f_{oc} relationships and measured f_{oc}
K_n	Measured for specific PFAS and NAPL	Estimated using QSPR, SPARC, or equivalent	Use measured or estimated K_{ow}
K_a	Measured for specific PFAS	Estimated using QSPR, SPARC, or equivalent	Estimated using aqueous solubility and vapor pressure
K_{aw}	Measured for specific PFAS and solution	Estimated using QSPR relationships	Estimated using representative solute
K_{nw}	Measured for specific PFAS and NAPL	Estimated using QSPR relationships	Estimated using representative solute
K_{an}	Measured for specific PFAS and NAPL	Estimated using QSPR relationships	Estimated using representative solute
A_{aw}	Measured for specific soil at relevant air saturation	Estimated using an interfacial area prediction correlation and measured solid surface area, soil texture, and air saturation	Estimated using median grain diameter correlation
A_{nw}	Measured for specific soil at relevant NAPL saturation	Estimated using an interfacial area prediction correlation and measured solid surface area, soil texture, and NAPL saturation	Estimated using median grain diameter correlation
A_{an}	Measured for specific soil at relevant air and NAPL saturations	Estimated using an interfacial area prediction correlation and measured solid surface area, soil texture, and NAPL saturation	Estimated using median grain diameter correlation
ρ_b	Measured	Estimated from soil type	–
θ_w	Measured	Estimated from soil type	–
θ_a	Measured	Determined from $\theta_a = n\text{-}\theta_w\text{-}\theta_n$	–
θ_n	Measured	Estimated from soil type	–
n	Measured	Estimated from soil type	–

Note: The methods are tiered, with Method 1 providing the greatest accuracy and confidence.

2.2.1. Solid-phase adsorption (K_d)

Distributed-component sorption models have been used to provide accurate predictions of K_d for many different compounds of interest (e.g., Luthy et al., 1997). These models are based on determining the adsorption potential of the compound for each relevant component of the soil (organic carbon, oxides, clays, silica), based on physicochemical properties of the compound. Higgins and Luthy (2007a,b) developed a mechanistically based model using this approach to predict the solid-phase sorption of perfluoroalkyl carboxylates, perfluoroalkyl sulfonates, and linear alkylbenzene sulfonates. The model included adorption via both hydrophobic and electrostatic processes and estimates the contribution of each to the adsorption coefficient using Gibbs free energy terms. The model was demonstrated to accurately predict the measured K_d values for all three classes of surfactants tested. This approach is used for the Method 2 estimation of K_d in Table 1. It requires knowledge of the soil components and basic physicochemical properties of the PFAS of interest.

Method 3 estimation is based on simple empirical relationships, such as $K_d = f_{oc}K_{oc}$, where K_{oc} is the organic-carbon normalized adsorption coefficient and f_{oc} is the fraction of soil organic carbon. K_{oc} is obtained either by measurement, from the literature, or by estimation (such as using K_{oc}-K_{ow} correlations). This approach is widely used to estimate K_d values for many compounds. However, it should be used with caution for PFAS, as other components of the porous media may contribute significantly to adsorption.

2.2.2. Partitioning to NAPL (K_n)

The widely used LFER-based estimation methods noted above is used for Method 2 in Table 1. The Method 3 approach is based on using K_{ow} values as a surrogate for K_n. It is cautioned that this approach may introduce significant additional uncertainty as measuring K_{ow} values for PFAS is more complex than for typical organics and the values may not be representative of actual partitioning behavior under relevant subsurface conditions (e.g., Goss et al., 2006).

2.2.3. Partitioning to air (K_a)

Measured Henry's coefficients are available for a large number of PFAS (e.g., Ding and Peijnenburg, 2013). Absent measured values, QSPR and SPARC based-approaches can be employed to estimate Henry's coefficients for PFAS. This approach is used for Method 2 in Table 1. The Method 3 approach is based on using reported vapor pressures and aqueous solubilities to estimate K_a values.

2.2.4. Interfacial adsorption coefficients (K_{aw}, K_{an}, and K_{nw})

Measured surface-tension or interfacial-tension data can be used to determine fluid-fluid interfacial adsorption coefficients. Adsorption at fluid-fluid interfaces is a function of the physico-chemical properties of the constituent. Thus, QSPR based-approaches can be used to estimate interface adsorption coefficients (e.g., Costanza and Brusseau, 2000). For example, Lyu et al. (2018) presented a QSPR model to predict air-water interfacial adsorption coefficients for PFAS, as noted above. These methods are incorporated for Method 2 estimation. Method 3 estimation employs interfacial adsorption coefficients obtained for surrogate interface tracers that have been previously reported in the literature.

2.2.5. Magnitude of interfacial area (A_{aw}, A_{an}, and A_{nw})

Prior research has demonstrated that fluid-fluid interfacial area is a function of soil properties and conditions, and is operationally dependent upon the measurement method. Peng and Brusseau (2005) developed a correlation equation to predict interfacial area as a function of soil texture:

$$A_i = s\left[1 + (\alpha(S_w))^n\right]^{-m} \quad (2)$$

where: $n = \frac{1}{2-m}$, $\alpha = 14.3\ln(U) + 3.72$, and $m = \begin{cases} -0.098U + 1.53 & U < 3.5 \\ 1.2 & U \geq 3.5 \end{cases}$ and U is uniformity coefficient (representing soil texture), S_w is wetting-phase saturation, and s is specific solid surface area. Interfacial area can be predicted using only three parameters: (1) specific surface area, which can be measured by N_2/BET analysis or estimated geometrically ($s = 6(1\text{-}n)/d$), where d is median grain diameter), (2) uniformity coefficient, obtained from a simple particle-size distribution test (sieve analysis), and (3) water saturation. This approach is used for Method 2 estimation.

Method 3 estimation is based on a simplified correlation of interfacial area to median grain diameter, as observed in several studies (Cho and Annable, 2005; Brusseau et al., 2009, 2010). For this approach, A_i is assumed to be a linear function of S_w as described by:

$$A_i = A_{max}(1\text{-}S_i) \quad (3)$$

where A_i is A_{aw}, A_{an}, or A_{nw}, A_{max} is the maximum fluid-fluid interfacial area associated with vanishingly small S_i, and S_i is saturation of the wetting phase. Water is the presumed wetting phase for all cases except for air-NAPL interfacial adsorption, in which case NAPL is presumed to be wetting. A_{max} has been shown to be a function of inverse grain diameter (Brusseau et al., 2009, 2010). Lyu et al. (2018) presented a regression equation based on A_{max} values measured from aqueous interfacial partitioning tracer tests, which use a surfactant as the interface tracer. It is anticipated that the interfacial areas measured with this method will be representative of the effective area influencing transport of many PFAS. The equation is given as: $A_{max} = 3.9\,d^{-1.2}$, with d the median grain diameter in cm.

3. Materials and methods for experiments

3.1. Materials

PFOS was selected as the representative PFAS used for the experiments. It was purchased from Sigma-Aldrich (CAS# 1763-23-1, 98%). PFOA (CAS#335-67-1, 98%) was used for a subset of the experiments and was purchased from AIKE Reagent (China). Both compounds have low vapor pressures and thus partitioning to the soil-vapor phase will be minimal for the conditions of these experiments (Brusseau, 2018). Pentafluorobenzoic acid (99%) was used as the nonreactive tracer, and was purchased from Strem Chemicals (Newburyport MA). This compound is not a PFAS and is not a surfactant. It has been widely used as a non-reactive tracer for transport studies with a diverse range of porous media.

The experiments conducted with the sand used 0.01 M NaCl as the background electrolyte. A synthetic groundwater solution (SGW) was used for the experiments conducted with the soil. The major cations in this synthetic groundwater (and concentration, mg/L) are Na^{+1} (50), Ca^{+2} (36), Mg^{+2} (25), and major anions are NO_3^{-1} (6), Cl^{-1} (60), CO_3^{-2}/HCO_3^{-1} (133), and SO_4^{-2} (99). The pH and ionic strength of the groundwater solution are 7.7 and 0.01 M, respectively. Solutions were prepared using distilled, deionized water.

PFOA and PFOS input concentrations (C_0) of 1 mg/L were used for the air-water miscible-displacement experiments conducted with the sand. A higher C_0 of 10 mg/L was used for the experiments conducted with the soil to reduce overall retention for purposes of the experimental apparatus discussed below. A C_0 of 10 mg/L was also used for the NAPL-water experiments. These concentrations are in the upper range of PFAS concentrations reported for groundwater. For example, a concentration greater than 6 mg/L was reported for PFOA at Fallon NAS, and a concentration greater than 2 mg/L was reported for PFOS at Tyndall AFB (Schultz et al., 2004). Given the high concentrations of PFAS reported for soil samples collected from some field sites, it is likely that concentrations in soil-pore water will be even higher for some vadose-zone source zones. For example, PFOS concentrations ranging up to 4 and 36 mg/kg were reported for samples collected at two fire-training areas (McGuire et al., 2014; Baduel et al., 2017).

Commercially available natural quartz sand (Accusand, UNIMIN Corp.) and a surface soil with moderate organic-carbon content were used in all column experiments. The sand has a median grain diameter of 0.35 mm and a Uniformity coefficient of 1.1. It has a total organic carbon content of 0.04%, negligible clay, and Fe, Mn, and Al oxide contents of 14, 2.5, and 12 μg/g, respectively. The Eustis soil (siliceous, thermic Psammentic Paleudults) has a median grain diameter of 0.27 mm and a Uniformity coefficient of 2.3. It has a total organic-carbon content of 0.38%, composed of approximately 37% hard carbon (kerogen and black carbon) and 63% soft carbon (humic/fulvic acids, lipids). It also contains 1.7% clay mineral content (essentially all kaolinite), 0.5% feldspar, and Fe, Mn, and Al oxide contents of 314, 19, and 694 μg/g, respectively.

The columns used in this study were constructed of acrylic or stainless steel to minimize interaction with PFAS, and were 15 cm long with inner diameter of ~2.5 cm. Porous plates were placed in contact with the porous media on the top and at the bottom of the column to help promote uniform fluid distribution and to support the media. Precision HPLC pumps were used to provide fluid flow. A custom vacuum chamber and vacuum pump system was used for the majority of the air-water unsaturated-flow experiments. A high-precision syringe pump was used for introducing decane into the columns for the NAPL-water experiments. As noted below, analysis of background samples collected from the column effluent revealed the absence of any interferences associated with the column or apparatus for PFAS determination.

3.2. Surface-tension measurements

The surface and interfacial tensions of aqueous PFOS solutions (with 0.01 M NaCl and SGW) were measured using a De Nouy ring tensionmeter (Fisherscientific, Surface Tensiomat 21) following standard methods (ASTM D1331- 89). The tensiometer was calibrated with a weight of known mass. Each sample was measured three times with the deviation between measurements less than 0.7%.

The measured surface and interfacial tensions for PFOS are presented in Fig. 2. The surface tension for PFOA was reported in Lyu et al. (2018). The air-water interfacial adsorption coefficient and the NAPL-water interfacial adsorption coefficient can be determined from the surface-tension and interfacial-tension functions, respectively. The surface excess Γ (mol/cm^2) is related to aqueous phase concentration (C) using the Gibbs equation:

$$\Gamma = \frac{-1}{RT}\frac{\partial\gamma}{\partial\, lnC} = K_i C \quad (4)$$

$$K_i = \frac{\Gamma}{C} = \frac{-1}{RTC}\frac{\partial\gamma}{\partial\, lnC} \quad (5)$$

where K_i represents the interfacial adsorption coefficient (in our case K_{aw} or K_{nw}, cm), γ is the interfacial tension (dyn/cm or mN/m), C represents the aqueous phase concentration (mol/cm^3), T is temperature (°K), and R is the gas constant (erg/mol °K). The surface-tension and interfacial-tension data measured for this work were analyzed using methods described previously to obtain K_{aw} and K_{nw} (Kim et al., 1997; Brusseau et al., 2007, 2015).

3.3. Miscible-displacement experiments

The columns were packed with air-dried sand or soil to obtain uniform bulk densities. The columns were oriented vertically for all experiments. Each column was first saturated with water by introducing water at a low flow rate (~0.05 mL/min) into the bottom of the column. Saturated-flow experiments were conducted with the nonreactive tracer to characterize the hydrodynamic properties of the packed columns. Experiments were then conducted with PFOA or PFOS to determine the retardation caused by solid-phase sorption. The experiments were conducted with a flow rate of 1 mL/min, equivalent to a mean pore-water velocity of ~30 cm/h.

To initiate the air-water unsaturated-flow experiments for PFOS, tubing from the bottom of the column was connected to a vacuum chamber that housed a fraction collector to which the column effluent line was connected. The chamber was connected to a vacuum pump. A HPLC pump was used to provide constant water flow to the exposed top of the column. A thin layer of glass beads was placed on top of the sand surface to help distribute solution and protect the surface from disruption. Manipulation of the injection flow rate and the magnitude of vacuum provides for controlled drainage to a selected water content. These methods have been demonstrated in our prior work to produce uniform water-content distributions (e.g., Brusseau et al., 2007, 2015). Once steady state conditions were achieved, miscible-displacement experiments were conducted for the nonreactive tracer and PFOS. The water saturation was ~0.66. While this apparatus provides for precise flow control, the sample capacity of the fraction collector housed in the chamber limits the total length of a single experiment. Thus, higher C_0s were used for the experiments to reduce the overall magnitude of retardation (as PFOS retention via solid-phase sorption and particularly fluid-fluid interfacial adsorption is nonlinear), thereby reducing experiment length.

For PFOA, two pumps were connected to the column, one to the top where solution was injected and one to the bottom where solution was withdrawn. Differential rates of solution injection and extraction results in a change in water saturation under controlled conditions. Experiments were conducted for PFOA at a saturation of 0.78. Only arrival waves were measured for the PFOA experiments. The unsaturated-flow experiments were conducted with a flow rate of 0.5 mL/min, equivalent to a mean pore-water velocity of ~26 cm/h.

For the NAPL-water experiments, decane was first injected into the top of the vertically oriented water-saturated column for several pore volumes. Aqueous solution was then injected into the bottom of the column to displace the free-phase decane, leaving a residual saturation trapped by capillary forces. Volumes of decane injected and recovered, as well as changes in mass of the column, were measured to determine final saturations. Nonreactive tracer tests were conducted before and after emplacement of the decane to characterize the impact of NAPL saturation on solute transport.

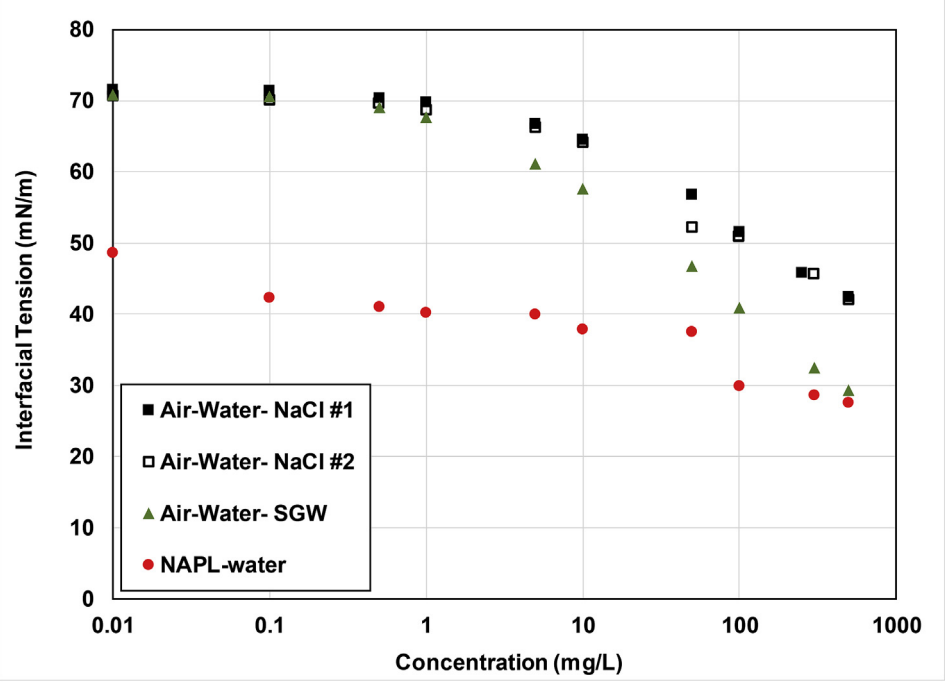

Fig. 2. Measured surface tensions for PFOS in water with 0.01 M NaCl or synthetic groundwater (SGW), and measured interfacial tension for PFOS in water with 0.01 M NaCl.

A batch experiment was conducted to measure the distribution coefficient, K_n, for PFOS partitioning into decane. Three initial concentrations were used, 2, 20 and 200 mg/L. These higher concentrations were employed to minimize the contribution of adsorption at the decane-water interface in the vials, given that K_{nw} decreases significantly with increasing aqueous concentration (eq (5)). Calculations revealed that the contribution of adsorption at the NAPL-water interface was less than 0.5% of total mass balance for the lowest initial concentration. Given that liquid-liquid partitioning is a linear process, the use of these concentrations to minimize complications from interfacial adsorption is anticipated to provide more robust results compared to the use of much lower concentrations. The experiment was conducted in triplicate, with accompanying controls containing no decane. A mean K_n of 0.02 was determined from the experiment, with a 95% confidence interval spanning zero. This indicates that there was minimal measurable partitioning of PFOS into decane for the conditions employed.

Measured retardation factors were determined for each miscible-displacement experiment by the standard methods of calculating the area above the breakthrough curve and by moment analysis. Their uncertainty, related to uncertainty in concentration and flow rate, is relatively small for these controlled experiments. These retardation factors incorporate the contributions of all relevant retention processes influencing transport. Retardation factors predicted using the methods outlined in the previous section will be compared to the measured values. The fractions of total retention for the relevant retention process are calculated to evaluate their relative significance. This is calculated as follows, using air-water interfacial adsorption (F_{awia}) as the example: $F_{awia} = (K_{aw}A_{aw}/\theta_w)/(R-1)$.

A one-dimensional solute-transport model incorporating nonlinear adsorption was used to simulate the full nonreactive tracer and PFOS breakthrough curves (e.g., Hu and Brusseau, 1998). The Peclet number was optimized by curve-fitting to the nonreactive tracer breakthrough curve. The measured retardation factors are used to produce predicted breakthrough curves.

3.4. Analytical methods

The nonreactive tracer samples were analyzed by ultraviolet–visible spectrophotometry at 262 nm wavelength. PFOS and PFOA samples were analyzed by two methods. The first method employed High Performance Liquid Chromatography tandem mass spectrometry. PFOS analysis employed a Waters Alliance 2695 LC coupled to a Micromass Quatrro Ultima Triple Quadrupole MS system, using negative electrospray ionization (ESI-). A Thermoscientific Betasil™ C18, 2.1 × 150 mm, 5 μm particle size analytical column was used. Aqueous samples were injected directly, with injection volumes of 20 μL. Eluents A and B were water + 5 mM ammonium acetate and 90% acetonitrile + 10% water + 5 mM ammonium acetate respectively. Elution was performed with a flow rate of 0.2 mL/min isocratically for 1 min at 20% eluent B and then a linear gradient to 100% B in 8 min, and finally isocratically for 3 min at 100% eluent B. The column was re-equilibrated for 7 min at initial conditions. Column temperature was maintained at 30 °C. PFOA was analyzed using an Agilent Model 1100 LC coupled to a TSQ quantum (Thermo Scientific) tandem MS system. The dual mobile phase comprised 5 mM ammonium acetate and acetonitrile applied in a 60:40 gradient at a flow rate of 0.2 mL/min. The aqueous samples were injected directly, with injection volumes of 2 μL. Retention time was consistently ~4.3 min. The column was an Agilent C18 maintained at 40 °C.

Standard QA/QC protocols were employed. Blanks, background samples, and check standards were analyzed periodically for each sample set. The results for the first two were lower than the quantifiable detection limit. The coefficients of determination (r^2) for the calibration curves were larger than 0.99 and 0.999 for PFOS and PFOA, respectively. The quantifiable detection limits are ~1 μg/L for PFOS and ~0.5 μg/L for PFOA. Background aqueous samples collected from the column effluent before injection of PFAS revealed no measurable concentrations or other interferences for all experiments.

The second method employed the methylene blue active substances (MBAS) assay (e.g., Chitikela et al., 1995). This method was used for the experiments conducted for the soil and the NAPL-water system. This is a standard method used to quantify anionic surfactant concentrations (ASTM D2330-02). It has been used successfully for determination of PFAS compounds under conditions wherein a single PFAS is present (Sharma et al., 1989; Moody and Field, 2000). The detailed explanation of the method is provided in the references cited. The quantifiable detection limit is ~0.4 mg/L for PFOS.

4. Results and discussion

4.1. Transport experiments

The transport of the nonreactive tracer was ideal for both saturated-flow and unsaturated-flow conditions, with sharp arrival and elution waves (minimal spreading), and retardation factors of 1 (see Fig. 3 through 6). The results obtained for the nonreactive tracer tests indicate that the columns were well-packed and that water flow was uniform, with no significant preferential flow or presence of no-flow domains.

The breakthrough curves for PFOS and PFOA transport in the sand under saturated-flow conditions are presented in Figs. 3 and 4, respectively. The breakthrough curves are relatively sharp and symmetrical, consistent with the results of the nonreactive tracer tests. Measured retardation factors of 1.3 and 1.8 are determined from the data for PFOA and PFOS, respectively (Table 2). These translate to K_d values of 0.08 and 0.15 L/kg for PFOA and PFOS, respectively. The relatively small magnitudes are to be expected given the nature of the sand. The larger value for PFOS compared to PFOA is consistent with results reported in the literature. The retardation factor for PFOS transport in the soil under saturated conditions was 3.6 (Fig. 5), with a resultant K_d of 0.56 L/kg. The larger value for the soil compared to the sand is consistent with the properties of the two media.

The breakthrough curves for the air-water experiments conducted under unsaturated conditions are shifted noticeably to the right of the breakthrough curves obtained under saturated conditions, indicating greater retardation (see Figs. 3–5). For PFOS transport in the sand, the retardation factor is 7 for a saturation of 0.66, compared to 1.8 for saturated conditions (Table 2). For PFOA, the retardation factor is 1.8 for a saturation of 0.78, compared to 1.3 for saturated conditions. The retardation factor for PFOS transport in the soil under unsaturated conditions ($S_w = 0.66$) is 7.3, compared to 3.6 for saturated conditions.

The greater retardation observed for unsaturated conditions is attributable to the impact of adsorption at the air-water interface on retention. Air-water interfacial adsorption is a significant source of retention for PFOS and PFOA in these systems, contributing 83 and 53% to total retention, respectively, for the sand, and 32% for PFOS retention in the soil. The relative contribution of air-water interfacial adsorption is observed to be lower for the soil, which is to be anticipated given the greater significance of solid-phase sorption and the use of a higher C_0.

The K_{aw} values determined from the measured retardation factors are 0.016 and 0.0026 cm for PFOS and PFOA, respectively, for

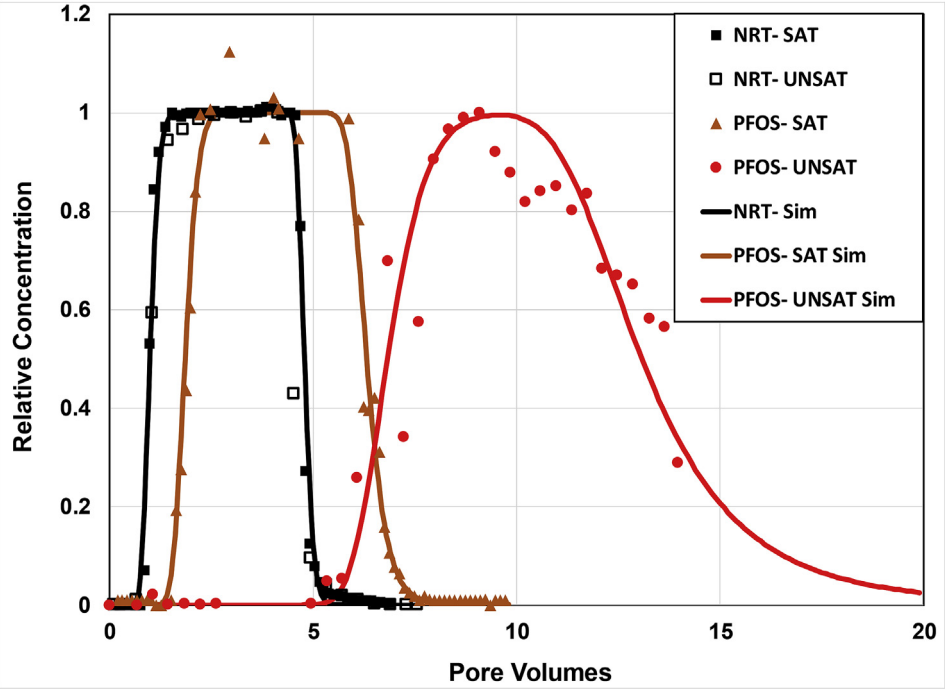

Fig. 3. Measured (symbols) and simulated (solid lines) breakthrough curves for transport of a nonreactive tracer (NRT) and PFOS under saturated (SAT) and unsaturated (UNSAT, $S_w = 0.66$) conditions in the sand. Simulations produced using a model that solves the one-dimensional advective-dispersive solute transport equation incorporating nonlinear adsorption.

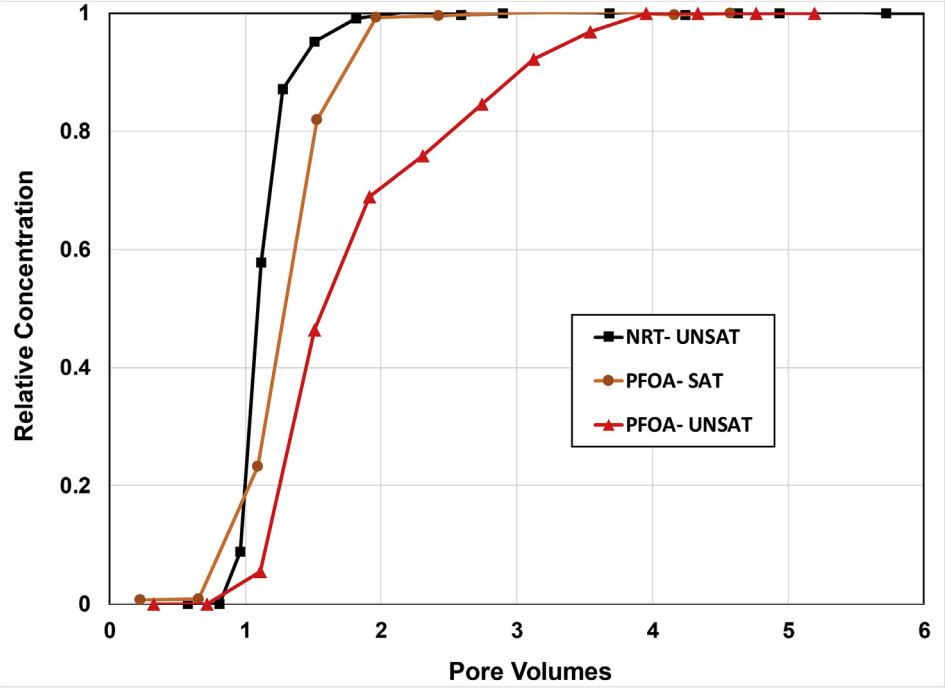

Fig. 4. Breakthrough curves for transport of a nonreactive tracer (NRT) and PFOA under saturated (SAT) and unsaturated (UNSAT, $S_w = 0.78$) conditions in the sand. The lines are for visualization purposes only. The NRT-SAT and PFOA-SAT data were originally reported in Lyu et al. (2018).

the sand. These values compare very well to the values determined from the surface-tension data, 0.02 and 0.0027, respectively. The K_{aw} value determined from the measured retardation factor for the soil is 0.005 cm, which is half of the value determined from the surface-tension data (0.01).

The breakthrough curves for PFOS transport in the sand with and without the presence of decane NAPL are presented in Fig. 6. The breakthrough curves exhibit greater retardation for the columns with decane present (2 versus 1.2). In this case, the additional retention is attributable to adsorption at the NAPL-water interface.

Table 2
Measured and predicted retardation factors for transport in the air-water systems.

Expt	Water Saturation	Measured R[a]	Predicted R[b]	System
PFOS- Sand	1	1.8	2.2 (1.7–2.6)	Air-Water
PFOS- Sand	0.66	7.0	9 (5–13)	Air-Water
PFOA- Sand	1	1.3	1.2 (1.1–1.3)	Air-Water
PFOA- Sand	0.78	1.8	1.7 (1.5–1.9)	Air-Water
PFOS- Soil	1	3.6	–	Air-Water
PFOS- Soil	0.66	7.3	9.7[c]	Air-Water

[a] Determined from analysis of measured breakthrough curve.
[b] 95% confidence interval in parentheses incorporating combined uncertainty in K_{oc}, K_{aw}, and A_{aw}.
[c] Confidence intervals not determined.

The K_{nw} values determined from the measured retardation factors for PFOS transport are 0.003 and 0.002 cm, which are similar to the value determined from the interfacial-tension data (0.003).

4.2. Evaluation of model predictions

The surface-tension data reported in Fig. 2 are analyzed to determine measured K_{aw} values as explained previously. This is employing Method 1 in Table 1. Values of 0.0027 (±0.005) and 0.02 (±0.01) cm are determined for PFOA and PFOS, respectively, for a concentration of 1 mg/L. Interestingly, these values are very similar to those back-calculated from the measured breakthrough curves, as noted above. This demonstrates that surface-tension data provide accurate K_{aw} values for transport applications.

Air-water interfacial areas have been measured in our prior research for the sand used in this project (Brusseau et al., 2007, 2015). An A_{max} value of 216 (±17) cm^{-1} is determined from these data. Employing the simple estimation method (#3 in Table 1) of $A_{aw} = A_{max}(1\text{-}S_w)$ produces air-water interfacial areas of 73 (0.66) and 47.5 (0.78) for the water saturations used in these experiments. The regression equation reported by Lyu et al. (2018) was used to estimate an A_{max} value of 297 cm^{-1} for the soil, which translates to an A_{aw} of 102 cm^{-1} for a water saturation of 0.66.

The simple estimation method (#3 in Table 1) of $K_d = f_{oc}{}^*K_{oc}$ is used to estimate K_d values for the sand. Ignoring the contribution of inorganic soil constituents to PFAS sorption is viable for this case given the nature of the porous medium. Mean K_{oc} values of 112 and 594 are used based on values reported in the literature for PFOA and PFOS, respectively (Higgins and Luthy, 2006; Milinovic et al., 2015). K_d values of 0.045 and 0.238 are estimated for PFOA and PFOS, respectively, using the reported K_{oc}s and the measured f_{oc}. With measured values for bulk density and water content, predicted retardation factors can now be determined (Table 2). Inspection of Table 2 reveals that the predicted retardation factors are similar to the measured values, with 95% confidence intervals encompassing the measured values. The similarity of predicted and measured retardation factors indicate that the model provided adequate representation of the retention processes for this system.

A good match is observed between the simulations produced with a solute-transport model incorporating nonlinear adsorption and the measured PFOS breakthrough curves for the sand (Fig. 3). For these simulations, the measured retardation factors were used, along with the Peclet Number obtained from the nonreactive tracer. Thus, no curve-fitting was employed, and the simulations therefore represent predicted curves. Significant arrival-wave tailing is observed for PFOS transport in the soil compared to the sand, indicating the influence of rate-limited mass transfer.

5. Conclusion

Miscible-displacement experiments were conducted to investigate PFOS and PFOA transport under saturated and unsaturated conditions. The breakthrough curves for the experiments conducted under unsaturated conditions were shifted noticeably rightward compared to the breakthrough curves obtained under saturated conditions, indicating greater retardation. This greater retardation is due to the impact of adsorption at the air-water

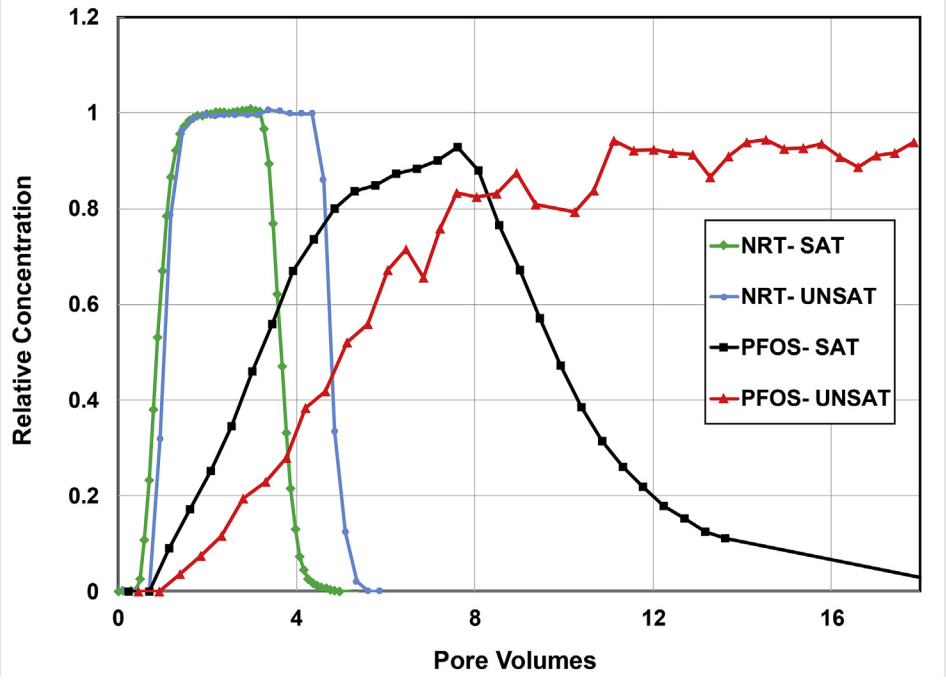

Fig. 5. Breakthrough curves for transport of a nonreactive tracer (NRT) and PFOS under saturated (SAT) and unsaturated (UNSAT, $S_w = 0.66$) conditions in the soil. The lines are for visualization purposes only.

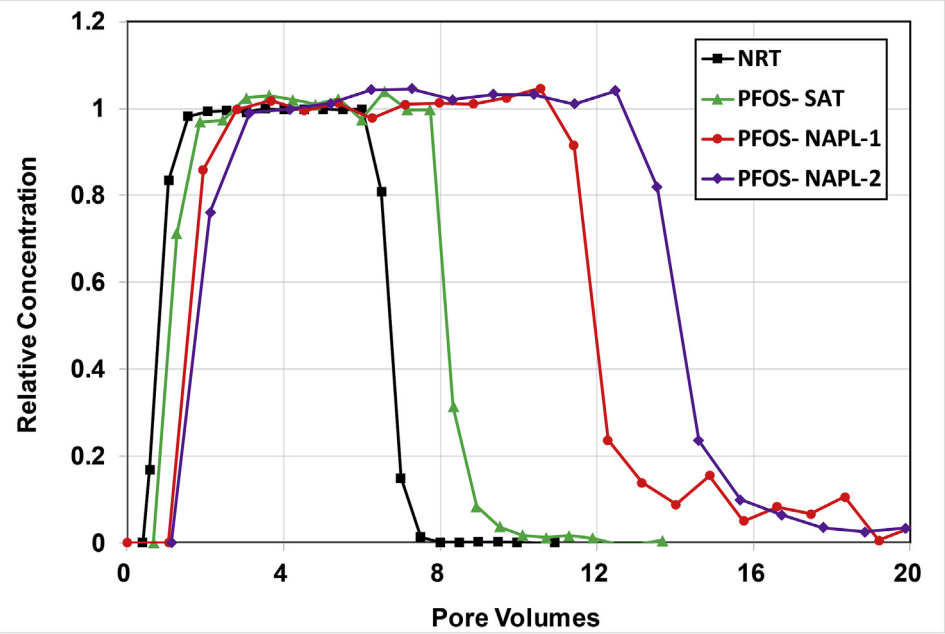

Fig. 6. Breakthrough curves for transport of PFOS in the absence (SAT) and presence of decane NAPL (NAPL, $S_w = 0.62$) in the sand. The nonreactive tracer (NRT) breakthrough curve shown is in the presence of decane. The lines are for visualization purposes only.

interface or NAPL-water interface on retention. Air-water and NAPL-water interfacial adsorption is a significant source of retention for PFOS and PFOA transport in the systems employed.

Selected methods were used to independently determine K_d, K_{aw}, and A_{aw} values to allow prediction of retardation factors for PFOS and PFOA. The predicted retardation factors were similar to the measured values. This demonstrates that the model provided adequate representation of the relevant retention processes, and that the parameter estimation methods produced reasonable values. The model should prove useful for predicting retardation factors for, and assessing the retention behavior of, PFAS in source zones.

PFAS consist of hundreds of compounds with different molecular structures, and they therefore comprise a range of physico-chemical properties. This greatly influences the magnitudes of distribution coefficients exhibited by individual compounds, and hence the relative importance of the various retention processes included in the comprehensive model presented herein. A given PFAS may not reside in all potential compartments, and different PFAS may reside in different subsets of compartments. The influence of PFAS properties on retention is accounted for in the model through the use of representative distribution coefficients for individual PFAS of interest, either measured or estimated. For example, a short-chain PFAS will undergo much less air-water interfacial adsorption than a longer-chain compound of the same homologous family in accordance with Traube's rule. This behavior is reflected in the much smaller K_{aw} value that would be determined for the shorter-chain compound from surface-tension measurements, as demonstrated by Lyu et al. (2018). Use of this smaller value in the model would produce a smaller retardation factor for the short-chain compound.

Distribution coefficients are also influenced by properties of the solution. For example, prior research has demonstrated that both K_d and K_{aw} for PFAS are influenced by ionic composition of solution and by the presence of co-contaminants. In addition, partitioning behavior for PFAS mixtures may deviate from that of single-component systems.

The magnitudes of retention and the relative importance of the various retention processes will also depend upon the magnitudes of the relevant phases present in the system of interest. The magnitude of air-water or NAPL-water interface present is the critical factor for adsorption at fluid-fluid interfaces. This is mediated by properties of the porous medium (texture) and system conditions (fluid contents). The magnitude of solid-phase adsorption will be governed by the soil organic-carbon content and, in some cases, the quantities of other soil constituents (clay minerals, metal oxides).

In addition, the relative significance of a given retention process is dependent upon the magnitudes of the other relevant retention processes. For example, it was observed herein that the relative contribution of air-water interfacial adsorption to total retention was less for the soil than for the sand, even though the soil has a greater magnitude of air-water interfacial area. The lesser relative significance of air-water interfacial adsorption for the soil was due in part to the greater magnitude of solid-phase adsorption for the soil, as well as the use of a larger C_0.

The model was tested herein for two-phase conditions representing a vadose-zone source devoid of NAPL, and a saturated-zone source containing NAPL. Future research should investigate retention of PFAS in three-phase systems containing NAPL and air, representing a vadose-zone source containing DNAPL. Prior research has shown that air-water, NAPL-water, and air-NAPL interfaces occur in such systems (Schnaar and Brusseau, 2006; Carroll et al., 2015), which would increase the complexity of PFAS retention.

Competing interest statement

The authors have no competing interests for this work.

Acknowledgements

This work was supported by the NIEHS Superfund Research Program (grant# P42 ES04940) and NSF EPSCoR (grant# IIA-1301346). We thank the reviewers for their constructive comments.

References

Ahrens, L., 2011. Polyfluoroalkyl compounds in the aquatic environment: a review of their occurrence and fate. J. Environ. Monit. 13, 20–31.

Anderson, R.H., Long, G.C., Porter, R.C., Anderson, J.K., 2016. Occurrence of select perfluoroalkyl substances at U.S. Air Force aqueous film-forming foam release sites other than fire-training areas: field-validation of critical fate and transport properties. Chemotherapy 150, 678–685.

Arp, H.P.H., Niederer, C., Goss, K.-U., 2006. Predicting the partitioning behavior of various highly fluorinated compounds. Environ. Sci. Technol. 40, 7298–7304.

Baduel, C., Mueller, J.F., Rotander, A., Corfield, J., Gomez-Ramos, M.-J., 2017. Discovery of novel per- and polyfluoroalkyl substances (PFASs) at a fire fighting training ground and preliminary investigation of their fate and mobility. Chemosphere 185, 1030–1038.

Bhhatarai, B., Gramatica, P., 2011. Prediction of aqueous solubility, vapor pressure and critical micelle concentration for aquatic partitioning of perfluorinated chemicals. Environ. Sci. Technol. 45, 8120–8128.

Brusseau, M.L., 2018. Assessing the potential contributions of additional retention processes to PFAS retardation in the subsurface. Sci. Total Environ. 613–614, 176–185.

Brusseau, M.L., Peng, S., Schnaar, G., Murao, A., 2007. Measuring air-water interfacial areas with x-ray microtomography and interfacial partitioning tracer tests. Environ. Sci. Technol. 41, 1956–1961.

Brusseau, M.L., Narter, M., Schnaar, S., Marble, J., 2009. Measurement and estimation of organic liquid/water interfacial areas for several natural porous media. Environ. Sci. Technol. 43, 3619–3625.

Brusseau, M.L., Narter, N., Janousek, H., 2010. Interfacial partitioning tracer test measurements of organic-liquid/water interfacial areas: application to soils and the influence of surface roughness. Environ. Sci. Technol. 44, 7596–7600.

Brusseau, M.L., El Ouni, A., Araujo, J.B., Zhong, H., 2015. Novel methods for measuring air-water interfacial area in unsaturated porous media. Chemotherapy 127, 208–213.

Carroll, K.C., McDonald, K., Marble, J., Russo, A.E., Brusseau, M.L., 2015. The impact of transitions between two-fluid and three-fluid phases on fluid configuration and fluid-fluid interfacial area in porous media. Water Resour. Res. 51, 7189–7201.

Chen, H., Chen, S., Quan, X., Zhao, Y.Z., Zhao, H.M., 2009. Sorption of perfluorooctane sulfonate (PFOS) on oil and oil-derived black carbon: influence of solution pH and [Ca2+]. Chemotherapy 77, 1406–1411.

Chitikela, S., Dentel, S.K., Allen, H.E., 1995. Modified method for the analysis of anionic surfactants as methylene blue active substances. Analyst 120, 2001–2004.

Cho, J.Y., Annable, M.D., 2005. Characterization of pore scale NAPL morphology in homogeneous sands as a function of grain size and NAPL dissolution. Chemosphere 61 (7), 899–908.

CONCAWE, 2017. Environmental Fate and Effects of Poly and Perfluoroalkyl Substances (PFAS). Network for Industrially Contaminated Land in Europe, CONCAWE.

Costanza, M., Brusseau, M.L., 2000. Influence of adsorption at the air-water interface on the transport of volatile contaminants in unsaturated porous media. Environ. Sci. Technol. 34, 1–11.

Cousins, I.T., Vestergren, R., Wang, Z., Scheringer, M., McLachlan, M.S., 2016. The precautionary principle and chemicals management: the example of perfluoroalkyl acids in groundwater. Environ. Int. 94, 331–340.

CRCCARE 2017, reportAssessment, Management and Remediation Guidance for Perfluorooctanesulfonate (PFOS) and Perfluorooctanoic Acid (PFOA) – Part 5: Management and Remediation of PFOS and PFOA, CRC CARE Technical Report no. 38, CRC for Contamination Assessment and Remediation of the Environment, Newcastle, Australia.

Ding, G., Peijnenburg, W.J.G.M., 2013. Physicochemical properties and aquatic toxicity of poly- and perfluorinated compounds. Crit. Rev. Environ. Sci. Technol. 43 (6), 598–678.

EPA (Environmental Protection Agency. 2016. FACT SHEET PFOA & PFOS Drinking Water Health Advisories. November 2016 EPA 800-F-16-003. U.S. Environmental Protection Agency, Washington, DC.

Goss, K., Bronner, G., Harner, T., Hertel, M., Schmidt, T.C., 2006. The partition behavior of fluorotelomer alcohols and olefins. Environ. Sci. Technol. 40, 3572–3577.

Guelfo, J.L., Higgins, C.P., 2013. Subsurface transport potential of perfluoroalkyl acids at aqueous film-forming foam (AFFF)-impacted sites. Environ. Sci. Technol. 47, 4164–4171.

Higgins, C.P., Luthy, R.G., 2006. Sorption of perfluorinated surfactants on sediments. Environ. Sci. Technol. 40, 7251.

Higgins, C.P., Luthy, R.G., 2007a. Modeling sorption of anionic surfactants onto sediment materials: an a priori approach for perfluoroalkyl surfactants and linear alkylbenzene sulfonates. Environ. Sci. Technol. 41, 3254–3261.

Higgins, C.P., Luthy, R.G., 2007b. Correction to: modeling sorption of anionic surfactants onto sediment materials: an a priori approach for perfluoroalkyl surfactants and linear alkylbenzene sulfonates. Environ. Sci. Technol. 41, 6316.

Hu, Q., Brusseau, M.L., 1998. Coupled effects of nonlinear, rate-limited sorption and biodegradation on transport of 2,4-dichlorophenoxyacetic acid in soil. Environ. Toxicol. Chem. 17, 1673–1680.

Kim, H., Rao, P.S.C., Annable, M.D., 1997. Determination of effective air–water interfacial area in partially saturated porous media using surfactant adsorption. Water Resour. Res. 33 (12), 2705–2711.

Krafft, M.P., Riess, J.G., 2015. Per- and polyfluorinated substances (PFAS): environmental challenges. Curr. Opin. Colloid Interface Sci. 20, 192–212.

Luthy, R.G., Aiken, G.R., Brusseau, M.L., Cunningham, S.D., Gschwend, P.M., Pignatello, J.J., Reinhard, M., Traina, S.J., Weber, W.J., Westall, J.C., 1997. Sequestration of hydrophobic organic contaminants by geosorbents. Environ. Sci. Technol. 31, 3341–3347.

Lyu, Y., Brusseau, M.L., Chen, W., Yan, N., Fu, X., Lin, X., 2018. Adsorption of PFOA at the air-water interface during transport in unsaturated porous media. Environ. Sci. Technol. 52, 7745–7753.

McGuire, M.E., Schaefer, C., Richards, T., Backe, W.J., Field, J.A., Houtz, E., Sedlak, D.L., Guelfo, J.L., Wunsch, A., Higgins, C.P., 2014. Evidence of remediation-induced alteration of subsurface poly- and perfluoroalkyl substance distribution at a former firefighter training area. Environ. Sci. Technol. 48 (12), 6644–6652.

McKenzie, E.R., Siegrist, R.L., McCray, J.E., Higgins, C.P., 2016. The influence of a non-aqueous phase liquid (NAPL) and chemical oxidant application on perfluoroalkyl acid (PFAA) fate and transport. Water Res. 92, 199–207.

Milinovic, J., Lacorte, S., Vidal, M., Rigol, A., 2015. Sorption behaviour of perfluoroalkyl substances in soils. Sci. Total Environ. 511, 63–71.

Moody, C.A., Field, J.A., 1999. Determination of perfluorocarboxylates in groundwater impacted by fire-fighting activity. Environ. Sci. Technol. 33, 2800–2806.

Moody, C.A., Field, J.A., 2000. Perfluorinated surfactants and the environmental implications of their use in fire-fighting foams. Environ. Sci. Technol. 34, 3864–3870.

Moody, C.A., Hebert, G.N., Strauss, S.H., Field, J.A., 2003. Occurrence and persistence of perfluorooctanesulfonate and other perfluorinated surfactants in groundwater at a fire-training area at Wurtsmith air force base, Michigan, USA. J. Environ. Monit. 5, 341–345.

NGWA (National Ground Water Association) 2017. Groundwater and Pfas: State of Knowledge and Practice. NGWA Press, Westerville, OH.

Peng, S., Brusseau, M.L., 2005. Impact of soil texture on air-water interfacial areas in unsaturated sandy porous media. Water Resour. Res. 41, W03021. https://doi.org/10.1029/2004WR003233.

Rayne, S., Forest, K., 2009. Perfluoroalkyl sulfonic and carboxylic acids: a critical review of physicochemical properties, levels and patterns in waters and wastewaters, and treatment methods. J. Environ. Sci. Health Part A 44, 1145–1199.

Schultz, M.M., Barofsky, D.F., Field, J.A., 2004. Quantitative determination of fluorotelomer sulfonates in groundwater by LC MS/MS. Environ. Sci. Technol. 38, 1828e1835. https://doi.org/10.1021/es035031j.

Schnaar, G., Brusseau, M.L., 2006. Characterizing pore-scale configuration of organic immiscible liquid in multiphase systems with synchrotron X-ray microtomography. Vadose Zone J. 5, 641–648.

Sharma, R., Pyter, R., Mukerjee, P., 1989. Spectrophotometric determination of perfluorocarboxylic acids (heptanoic to decanoic) and sodium perfluorooctanoate and decyl sulfate in mixtures by dye-extraction. Anal. Lett. 22, 999–1007.

Shin, H.M., Vieira, V.M., Ryan, P.B., Detwiler, R., Sanders, B., Steenland, K., Bartell, S.M., 2011. Environmental fate and transport modeling for perfluorooctanoic acid emitted from the Washington works facility in West Virginia. Environ. Sci. Technol. 45 (4), 1435–1442.

Weber, A.K., Barber, L.B., LeBlanc, D.R., Sunderland, E.M., Vecitis, C.D., 2017. Geochemical and hydrologic factors controlling subsurface transport of poly- and perfluoroalkyl substances, Cape Cod, Massachusetts. Environ. Sci. Technol. 51, 4269–4279, 2017.

Xiao, F., Simcik, M.F., Halbach, T.R., Gulliver, J.S., 2015. Perfluorooctane sulfonate (PFOS) and perfluorooctanoate (PFOA) in soils and groundwater of a U.S. metropolitan area: migration and implications for human exposure. Water Res. 72, 64–74.